*This full text paper was peer reviewed at the direction of IEEE Communications Society subject matter experts for publication in the WCNC 2007 proceedings.*

# Four-Group Decodable Semi-Orthogonal Algebraic Space-Time Block Codes

Dũng Ngọc Đào, Chintha Tellambura
ECE Department
University of Alberta
Edmonton, Alberta, Canada
{dndung, chintha}@ece.ualberta.ca

Chau Yuen, Tjeng Thiang Tjhung
Wireless Comms. Division
Institute for Infocomm Research
21 Heng Mui Keng Terrace, Singapore
{cyuen, tjhungtt}@i2r.a-star.edu.sg

Yong Liang Guan
School of EEE
Nanyang Technological University
Nanyang Avenue, Singapore
eylguan@ntu.edu.sg

***Abstract*— The rate-one semi-orthogonal algebraic space-time (SAST) codes is recently introduced. In this paper, we propose a new signal design method for SAST codes so that the transmitted symbols can be divided into four groups for maximum likelihood (ML) detection; we call this new design of SAST codes four-group decodable SAST (4Gp-SAST) codes. The decoding complexity of 4Gp-SAST codes is greatly reduced compared with that of the original SAST codes, where the ML decoding of the transmitted symbols is made into two groups. The exact pair-wise error probability of 4Gp-SAST codes is derived and it is used to optimize the signal designs. Simulation results show that 4Gp-SAST codes perform better than several low complexity space-time block codes such as orthogonal and quasi-orthogonal codes.**

## I. Introduction

Space-time block codes (STBC[1]) have been extensively studied [1]. Among various STBC proposed so far, orthogonal STBC (OSTBC) have been successfully applied in the third generation wireless communication systems [2]–[4]. The key features leading to the wide application of OSTBC are their minimum complexity maximum likelihood (ML) detection and full diversity. On the other hand, OSTBC have low code rate when the number of transmit antennas is more than 2 [5]. The rate of one symbol per channel use (pcu) exists for 2 transmit antennas [2], [5] and the rate is not more than 3/4 for more than two transmit antennas.

To achieve the higher data rates for future wireless systems, many research efforts have been made to the designs of high rate STBC, and at the same time, to keep the complexity low. Several quasi-orthogonal STBC (QSTBC) have been proposed (see, e.g [6]. These QSTBC allow joint maximum likelihood (ML) decoding of two complex symbols. However, the rate-one QSTBC can be designed for 4 transmit antennas only. Recently, several rate-one STBC for any number of transmit antennas have been proposed [7]–[10], in which the transmitted symbols can be completely separated into two blocks for ML detection. This feature greatly reduces the decoding complexity compared with that of the rate-one diagonal algebraic space-time (DAST) codes [11], [12].

The algebraic structure of STBC with single complex-symbol decoding has been revised [13], [14] enabling two new designs of single complex-symbol decodable STBC, namely coordinate interleaved orthogonal designs (CIOD) [13] and minimum decoding complexity QSTBC (MDC-QSTBC) [14]. Nevertheless, these codes offer the rate of one symbol pcu for 4 transmit antennas only. Yuen *et al.* [15] have tried to search for the high-rate STBC with low decoding complexity. They have found a code of rate 5/4 with full symbol-wise diversity [1] for 4 transmit antennas; this code allows the separation of transmitted symbols into two groups at the receiver.

Recently, the rate-one semi-orthogonal algebraic space-time (SAST) codes have been proposed in [10]. The SAST codes allow the separation of the transmitted symbols into 2 groups for ML detection. Furthermore, near capacity of multiple-input single-ouput (MISO) channels can be achieved by using SAST codes. Therefore, it is of interest to study other properties of SAST codes.

In this paper, we show that the transmitted symbols embedded in the SAST code matrix can be divided into four groups for ML detection. We thus call this code four-group decodable SAST (4Gp-SAST) codes. The exact pair-wise error probability (PEP) of 4Gp-SAST codes is derived. Based on the exact PEP, we optimize the signal rotation for the traditional constellations (such as quadrature amplitude modulation (QAM)) to obtain full diversity and the best performance. The 4Gp-SAST codes perform better than several existing low complexity codes such as OSTBC and QSTBC.

To provide a closer look on the new 4Gp-SAST codes, we compare their main parameters with several existing low-decoding complexity STBC for 6 antennas in Table I, including OSTBC, ABBA-QSTBC [6], MDC-QSTBC [14] and 4Gp-QSTBC [16]. Clearly, the new 4Gp-SAST codes offer several advantages such as higher code rate, lower encoding/decoding delay, and low decoding complexity. Moreover, from simulation results, our new codes also yield significant SNR gains compared with the OSTBC, QSTBC and MDC-QSTBC.

## II. System Model and Preliminaries

We first set the common notations to be used throughout the paper. Superscripts $^{\mathsf{T}}$, $^{*}$, and $^{\dagger}$ denote matrix transpose, conjugate, and transpose conjugate, respectively. The identity and all-zero square matrices of proper size are denoted by $\boldsymbol{I}$ and $\mathbf{0}$. The diagonal matrix with elements of vector $\boldsymbol{x}$

[1]The acronym STBC also stands for space-time block code/coding, depending on the context.

1525-3511/07/$25.00 ©2007 IEEE

TABLE I
COMPARISON OF SEVERAL LOW COMPLEXITY STBC FOR 6 ANTENNAS.

| Codes | Maximal rate | Delay | Real symbol decoding |
|---|---|---|---|
| OSTBC [5] | 2/3 | 30 | 1 or 2 |
| ABBA-QSTBC [6] | 3/4 | 8 | 4 |
| MDC-QSTBC [14] | 3/4 | 8 | 2 |
| QSTBC [7]–[9] | 1 | 8 | 8 |
| 4Gp-QSTBC [16] | 1 | 8 | 4 |
| SAST [10] | 1 | 6 | 6 |
| **4Gp-SAST** | **1** | **6** | **3** |

on the main diagonal is denoted by $\mathrm{diag}(\boldsymbol{x})$. $\|X\|_{\mathsf{F}}$ stands for Frobenius norm of matrix $X$ and $\otimes$ denotes Kronecker product [17]. $\mathbb{E}[\cdot]$ denotes average. A mean-$m$ and variance-$\sigma^2$ circularly complex Gaussian random variable is written by $\mathcal{CN}(m,\sigma^2)$. $\Re(X)$ and $\Im(X)$ denote the real and imaginary parts of $X$, respectively. Unless otherwise stated, all the vectors are column vectors and denoted by lowercase bold letters.

### A. System Model

We consider data transmission over a quasi-static Rayleigh flat fading channel, i.e. the channel is fixed for the duration of a codeword, but can vary from the duration of one codeword to another codeword. The transmitter and receiver are equipped with $M$ transmit (transmit) and $N$ receive (receive) antennas. The channel gain $h_{ik}$ $(i = 1,2,\cdots,M; k = 1,2,\cdots,N)$ between the $(i,k)$-th transmit-receive antenna pair is assumed to be $\mathcal{CN}(0,1)$. We assume no spatial correlation at either transmit or receive array, and the receiver, but not the transmitter, completely knows the channel gains.

The ST encoder parses data symbols into a $T \times M$ code matrix $X$ of an ST code $\mathcal{X}$ as follows:

$$X = \left[c_{ti}\right]_{i=1,\ldots,M}^{t=1,\ldots T} \tag{1}$$

where $c_{ti}$ is the symbol transmitted from antenna $i$ at time $t$ $(1 \le t \le T)$. The average energy of the code matrices is constrained such that $\mathcal{E}_{\mathcal{X}} = \sum_{i=1}^{M}\sum_{t=1}^{T}\mathbb{E}[|c_{ti}|^2] = T$.

The received signals $y_{lk}$ of the $k$th antenna at time $t$ can be arranged in a matrix $Y$ of size $T \times N$. Thus, one can represent the transmit-receive signal relation as

$$Y = \sqrt{\rho}XH + Z \tag{2}$$

where $H = [h_{ik}]$, and $Z = [z_{ik}]$ of size $T \times N$, and $z_{ik}$ are independently, identically distributed (i.i.d.) $\mathcal{CN}(0,1)$. The transmit power is scaled by $\rho$ so that the average signal-to-noise ratio (SNR) at each receive antenna is $\rho$, independent of the number of transmit antennas. However, $\rho$ is sometimes omitted for notational brevity.

The mapping of a block of $K$ data symbols $(s_1, s_2, \cdots, s_K)$ into a $T \times M$ code matrix can be represented in a general dispersion form [3], [18] as follows:

$$X = \sum_{k=1}^{K}\left(a_k A_k + b_k B_k\right) \tag{3}$$

where $A_k$ and $B_k$, $(k = 1,2,\cdots,K)$ are $T \times M$ complex-valued constant matrices; they are commonly called dispersion matrices. $a_k$ and $b_k$ are the real and imaginary parts of the symbol $s_k$.

In (3), there are totally $2K$ real variables $a_i$ and $b_i$. We can replace variables $a_i$ and $b_i$ (and their dispersion matrices $A_k$ and $B_k$) by the same symbolic variable $c_l$ (and dispersion matrix $C_l$). Then (3) becomes

$$X = \sum_{l=1}^{L} c_l C_l. \tag{4}$$

Denote the transmitted data vector $\boldsymbol{c} = \begin{bmatrix} c_1 & c_2 & \ldots c_L \end{bmatrix}^{\mathsf{T}}$. The ML decoding of STBC is to find the solution $\hat{\boldsymbol{c}}$ of the following metric:

$$\hat{\boldsymbol{c}} = \arg\min_{\mathbf{c}} \|Y - XH\|_{\mathsf{F}}^2 . \tag{5}$$

### B. Algebraic Constraints of QSTBC

In QSTBC we divide the $L$ (real) transmitted symbols embedded in a code matrix into $\Gamma$ independent groups, so that the ML detection of a transmitted code matrix can be decoupled into $\Gamma$ sub-metrics; each metric involves the symbols of only one group [6]–[10], [15]. We provide a definition of STBC with such feature to unify the notation in this paper as follows.

*Definition 1: A STBC is said to be* $\Gamma$*-group decodable if the ML decoding metric* (5) *can be decoupled into a linear sum of* $\Gamma$ *independent submetrics, each submetric consists of the symbols from only one group. The* $\Gamma$*-group decodable STBC is denoted by* $\Gamma$*Gp-STBC for short.*

Note that from Definition 1, the real and imaginary parts of the same complex symbol can belong to different groups.

In the most general case, we assume that there are $\Gamma$ groups; each group is denoted by $\Omega_i (i = 1,2,\ldots,\Gamma)$ and has $L_i$ symbols. Thus $L = \sum_{i=1}^{\Gamma} L_i$. Let $\Theta_i$ be the set of indexes of symbols in the group $\Omega_i$.

Yuen *et al.* [15, Theorem 1] have shown a sufficient condition for a STBC be multi-group decodable. In fact, this condition is also the necessary condition. We will state these results in the following theorem.

*Theorem 1: The necessary and sufficient conditions for a STBC to be* $\Gamma$*-group decodable are*

$$C_p^{\dagger} C_q + C_q^{\dagger} C_p = \mathbf{0} \quad \forall p \in \Theta_i, \forall q \in \Theta_j, i \ne j. \tag{6}$$

Theorem 1 covers [13, Theorem 9] (single-symbol decodable STBC) and can be proved similarly; details of proof are omitted for brevity.

## III. FOUR-GROUP DECODABLE SAST CODES

### A. Encoding

We first review the construction of SAST codes introduced in [10]. The SAST code matrix is constructed for $M = 2m$ transmit antennas using circulant blocks. Two data vectors $\boldsymbol{s}_1 = \begin{bmatrix} s_1 & s_2 & \ldots & s_m \end{bmatrix}^{\mathsf{T}}$ and $\boldsymbol{s}_2 =$

$\begin{bmatrix} s_{m+1} & s_{m+2} & \dots & s_{2m} \end{bmatrix}^{\mathsf{T}}$ are used to generate two circulant matrices [19]:

$$\mathcal{C}(\boldsymbol{s}_1^{\mathsf{T}}) = \begin{bmatrix} s_1 & s_2 & \dots & s_m \\ s_m & s_1 & \dots & s_{m-1} \\ \vdots & \vdots & \ddots & \vdots \\ s_2 & s_3 & \dots & s_1 \end{bmatrix},$$

$$\mathcal{C}(\boldsymbol{s}_2^{\mathsf{T}}) = \begin{bmatrix} s_{m+1} & s_{m+2} & \dots & s_{2m} \\ s_{2m} & s_{m+1} & \dots & s_{2m-1} \\ \vdots & \vdots & \ddots & \vdots \\ s_{m+2} & s_{m+3} & \dots & s_{m+1} \end{bmatrix}. \quad (7)$$

The SAST code matrix is constructed from as

$$\mathcal{S} = \begin{bmatrix} \mathcal{C}(\boldsymbol{s}_1) & \mathcal{C}(\boldsymbol{s}_2) \\ -\mathcal{C}^{\dagger}(\boldsymbol{s}_2) & \mathcal{C}^{\dagger}(\boldsymbol{s}_1) \end{bmatrix}. \quad (8)$$

For example, the SAST code for 6 transmit antennas is

$$\mathcal{S}_6 = \begin{bmatrix} u_1 & u_2 & u_3 & u_4 & u_5 & u_6 \\ u_3 & u_1 & u_2 & u_6 & u_4 & u_5 \\ u_2 & u_3 & u_1 & u_5 & u_6 & u_4 \\ -u_4^* & -u_6^* & -u_5^* & u_1^* & u_3^* & u_2^* \\ -u_5^* & -u_4^* & -u_6^* & u_2^* & u_1^* & u_3^* \\ -u_6^* & -u_5^* & -u_4^* & u_3^* & u_2^* & u_1^* \end{bmatrix}. \quad (9)$$

In order to use the general form of STBC (4) for SAST codes, we introduce a representation of circulant matrices using a matrix called *forward shift permutation* denoted by $\pi$ [19]. The definition of an $m \times m$ matrix $\pi$ is given below

$$\pi = \begin{bmatrix} 0 & 1 & 0 & 0 & \cdots & 0 \\ 0 & 0 & 1 & 0 & \cdots & 0 \\ \vdots & \vdots & \vdots & \vdots & \vdots & \vdots \\ 1 & 0 & 0 & 0 & \cdots & 0 \end{bmatrix}. \quad (10)$$

The circulant matrices $\mathcal{C}(\boldsymbol{s}_1)$ and $\mathcal{C}(\boldsymbol{s}_2)$ can be represented as

$$\mathcal{C}(\boldsymbol{s}_1^{\mathsf{T}}) = \sum_{i=1}^{m} s_i \pi^{i-1}, \qquad \mathcal{C}(\boldsymbol{s}_2^{\mathsf{T}}) = \sum_{i=1}^{m} s_{m+i} \pi^{i-1}. \quad (11)$$

The SAST code matrix follows

$$\mathcal{S} = \sum_{i=1}^{m} \Bigg( a_i \underbrace{\begin{bmatrix} \pi^{i-1} & \mathbf{0} \\ \mathbf{0} & (\pi^{\mathsf{T}})^{i-1} \end{bmatrix}}_{C_i} + b_i \underbrace{\begin{bmatrix} \mathsf{j}\,\pi^{i-1} & \mathbf{0} \\ \mathbf{0} & -\mathsf{j}(\pi^{\mathsf{T}})^{i-1} \end{bmatrix}}_{C_{m+i}}$$
$$+ a_{m+i} \underbrace{\begin{bmatrix} \mathbf{0} & \pi^{i-1} \\ -(\pi^{\mathsf{T}})^{i-1} & \mathbf{0} \end{bmatrix}}_{C_{2m+i}} + b_{m+i} \underbrace{\begin{bmatrix} \mathbf{0} & \mathsf{j}\,\pi^{i-1} \\ \mathsf{j}(\pi^{\mathsf{T}})^{i-1} & \mathbf{0} \end{bmatrix}}_{C_{3m+i}} \Bigg). \quad (12)$$

One can recognize that there are 4 groups of symbols: Group 1 with symbols $a_i$, group 2 with symbols $b_i$, group 3 with symbols $a_{m+i}$, group 4 with symbols $b_{m+i}$ $(i = 1, 2, \dots, m)$. We can show that these four groups can be decoded separately using Theorem 1.

*Theorem 2: By construction* (8)*, SAST codes are four-group decodable.*

Compared with 4Gp-QSTBC [16], 4Gp-SAST codes also have rate of one symbol pcu. The main different of the two codes is their delay-optimality. While 4Gp-QSTBC is delay-optimal if the number of transmit antennas is a power of 2, SAST codes are delay-optimal for $2m$ transmit antennas.

Theorem 2 can be shown explicitly using Theorem 1. Due to the space limit, we ommit the proof. However, we will derive a new ML decoder such that the decoding of transmitted symbols becomes the decoding of 4 orthogonal groups instead.

### *B. Decoder of 4Gp-SAST codes*

Applying the general ML decoder in (5), the decoding of transmitted symbols of 4Gp-SAST codes becomes the decoding of 4 vectors: $\Re(\boldsymbol{s}_1), \Im(\boldsymbol{s}_1), \Re(\boldsymbol{s}_2)$ and $\Im(\boldsymbol{s}_2)$. However, this approach results in exponential decoding complexity. We therefore will derive an alternative decoder for 4Gp-SAST codes in order to provide more insights into the structure of the equivalent channel for 4Gp-SAST codes. Furthermore, the equivalent channel can be used to analyze the codes' performance and to apply sphere decoding [20].

The derivation of the decoder for 4Gp-SAST codes requires two steps. The first step is to decouple the two data vectors $\boldsymbol{s}_1$ and $\boldsymbol{s}_2$. In the second step, the real and imaginary parts of vectors $\boldsymbol{s}_1$ and $\boldsymbol{s}_2$ will be separated. The first decoding step has been described in [10] and will be briefly reviewed in the following. We provide the details of the decoder with one receive antennas and generalization for multiple receive antennas can be easily developed.

We introduce another type of circulant matrix called left ciculant, denoted by $\mathcal{C}_L(\boldsymbol{x})$, where the $i$th row is obtained by circular shifts $(i-1)$ times to the left the row vector $\boldsymbol{x}$.

$$\mathcal{C}_L(\boldsymbol{x}) = \begin{bmatrix} x_1 & x_2 & \dots & x_m \\ x_2 & x_3 & \dots & x_1 \\ \vdots & \vdots & \ddots & \vdots \\ x_m & x_1 & \dots & x_{m-1} \end{bmatrix}. \quad (13)$$

Let us define a permutation $\Pi$ on an arbitrary matrix $X$ such that, the $(m-i+2)$th row is permuted with the $i$th row for $i = 2, 3, ..., \lceil \frac{m}{2} \rceil$, where $\lceil(\cdot)\rceil$ is ceiling function. One can verify that

$$\Pi(\mathcal{C}_L(\boldsymbol{x})) = \mathcal{C}(\boldsymbol{x}). \quad (14)$$

This useful operator will be used for our next derivation.

Let $\boldsymbol{y} = \begin{bmatrix} \boldsymbol{y}_1^{\mathsf{T}} & \boldsymbol{y}_2^{\mathsf{T}} \end{bmatrix}^{\mathsf{T}}$, $\boldsymbol{y}_1 = \begin{bmatrix} y_1 & y_2 & \dots & y_m \end{bmatrix}^{\mathsf{T}}$, $\boldsymbol{y}_2 = \begin{bmatrix} y_{m+1} & y_{m+2} & \dots & y_M \end{bmatrix}^{\mathsf{T}}$, $\boldsymbol{h} = \begin{bmatrix} \boldsymbol{h}_1^{\mathsf{T}} & \boldsymbol{h}_2^{\mathsf{T}} \end{bmatrix}^{\mathsf{T}}$, $\boldsymbol{h}_1 = \begin{bmatrix} h_1 & h_2 & \dots & h_m \end{bmatrix}^{\mathsf{T}}$, $\boldsymbol{h}_2 = \begin{bmatrix} h_{m+1} & h_{m+2} & \dots & h_{2m} \end{bmatrix}^{\mathsf{T}}$, $\boldsymbol{z} = \begin{bmatrix} \boldsymbol{z}_1^{\mathsf{T}} & \boldsymbol{z}_2^{\mathsf{T}} \end{bmatrix}^{\mathsf{T}}$, $\boldsymbol{z}_1 = \begin{bmatrix} z_1 & z_2 & \dots & z_m \end{bmatrix}^{\mathsf{T}}$, $\boldsymbol{z}_2 = \begin{bmatrix} z_{m+1} & z_{m+2} & \dots & z_{2m} \end{bmatrix}^{\mathsf{T}}$.

We can write the transmit-receive signal relation as

$$\begin{bmatrix} \boldsymbol{y}_1 \\ \boldsymbol{y}_2 \end{bmatrix} = \sqrt{\frac{\rho}{M}} \begin{bmatrix} \mathcal{C}(\boldsymbol{s}_1) & \mathcal{C}(\boldsymbol{s}_2) \\ -\mathcal{C}^{\dagger}(\boldsymbol{s}_2) & \mathcal{C}^{\dagger}(\boldsymbol{s}_1) \end{bmatrix} \begin{bmatrix} \boldsymbol{h}_1 \\ \boldsymbol{h}_2 \end{bmatrix} + \begin{bmatrix} \boldsymbol{z}_1 \\ \boldsymbol{z}_2 \end{bmatrix}. \quad (15)$$

Applying permutation $\Pi$ in (14) for the column matrix $\boldsymbol{y}_1$, we obtain [10]:

$$\begin{bmatrix}\bar{\boldsymbol{y}}_1\\ \bar{\boldsymbol{y}}_2\end{bmatrix} \triangleq \begin{bmatrix}\Pi(\boldsymbol{y}_1)\\ \boldsymbol{y}_2^*\end{bmatrix} = \sqrt{\frac{\rho}{M}} \underbrace{\begin{bmatrix}H_1 & H_2\\ H_2^\dagger & -H_1^\dagger\end{bmatrix}}_{\mathcal{H}} \begin{bmatrix}\boldsymbol{s}_1\\ \boldsymbol{s}_2\end{bmatrix} + \begin{bmatrix}\bar{\boldsymbol{z}}_1\\ \bar{\boldsymbol{z}}_2\end{bmatrix} \quad (16)$$

where $H_1 = \mathcal{C}(\boldsymbol{h}_1^\mathsf{T})$, $H_2 = \mathcal{C}(\boldsymbol{h}_2^\mathsf{T})$, $\bar{\boldsymbol{z}}_1 = \Pi(\boldsymbol{z}_1)$, $\bar{\boldsymbol{z}}_2 = \boldsymbol{z}_2^*$. The elements of $\bar{\boldsymbol{z}}_1$ and $\bar{\boldsymbol{z}}_2$ have the same statistics, $\mathcal{CN}(0,1)$, as elements of $\boldsymbol{z}_1$ and $\boldsymbol{z}_2$.

We now multiply $\mathcal{H}^\dagger$ to both sides of (16). Let $\hat{\mathcal{H}} = H_1^\dagger H_1 + H_2^\dagger H_2$, we get

$$\begin{aligned}\begin{bmatrix}\hat{\boldsymbol{y}}_1\\ \hat{\boldsymbol{y}}_2\end{bmatrix} &= \mathcal{H}^\dagger \begin{bmatrix}\bar{\boldsymbol{y}}_1\\ \bar{\boldsymbol{y}}_2\end{bmatrix} = \sqrt{\frac{\rho}{M}} \begin{bmatrix}\hat{\mathcal{H}} & \mathbf{0}_m\\ \mathbf{0}_m & \hat{\mathcal{H}}\end{bmatrix} \begin{bmatrix}\boldsymbol{s}_1\\ \boldsymbol{s}_2\end{bmatrix} + \mathcal{H}^\dagger \begin{bmatrix}\bar{\boldsymbol{z}}_1\\ \bar{\boldsymbol{z}}_2\end{bmatrix}\\ &= \sqrt{\frac{\rho}{M}} \begin{bmatrix}\hat{\mathcal{H}} & \mathbf{0}_m\\ \mathbf{0}_m & \hat{\mathcal{H}}\end{bmatrix} \begin{bmatrix}\boldsymbol{s}_1\\ \boldsymbol{s}_2\end{bmatrix} + \underbrace{\begin{bmatrix}\hat{\boldsymbol{z}}_1\\ \hat{\boldsymbol{z}}_2\end{bmatrix}}_{\hat{\boldsymbol{z}}}. \end{aligned} \quad (17)$$

The covariance matrix of the additive noise vector $\hat{\boldsymbol{z}}$ is

$$E[\boldsymbol{z}\boldsymbol{z}^\dagger] = \begin{bmatrix}\hat{\mathcal{H}} & \mathbf{0}_m\\ \mathbf{0}_m & \hat{\mathcal{H}}\end{bmatrix}. \quad (18)$$

Therefore, noise vectors $\hat{\boldsymbol{z}}_1$ and $\hat{\boldsymbol{z}_s}$ are uncorrelated and have the same covariance matrix $\hat{\mathcal{H}}$. Thus $\boldsymbol{s}_1$ and $\boldsymbol{s}_2$ can be decoded separately using $\hat{\boldsymbol{y}}_i = \hat{\mathcal{H}}\boldsymbol{s}_i + \hat{\boldsymbol{z}_i}$, $i = 1, 2$. The noise vectors $\hat{\boldsymbol{z}}_1$ and $\hat{\boldsymbol{z}}_s$ can be whitened by the same whitening matrix $\hat{\mathcal{H}}^{-1/2}$. The equivalent equations for transmit-receive signals are

$$\hat{\mathcal{H}}^{-1/2}\hat{\boldsymbol{y}}_i = \sqrt{\frac{\rho}{M}}\hat{\mathcal{H}}^{1/2}\boldsymbol{s}_i + \hat{\mathcal{H}}^{-1/2}\hat{\boldsymbol{z}}_i, \qquad i = 1, 2. \quad (19)$$

At this point, the decoding of SAST codes becomes the detection of 2 group of complex symbols $\boldsymbol{s}_i$ $(i = 1, 2)$. Our next step is to separate the real and imaginary parts of vectors $\boldsymbol{s}_i$ by exploiting the properties of $\hat{\mathcal{H}}$.

Recall that $\hat{\mathcal{H}} = H_1^\dagger H_1 + H_2^\dagger H_2$, and both $H_1$ and $H_2$ are circulant. Hence, $\hat{\mathcal{H}}$ is also circulant [19]. Let $\Lambda_i = \begin{bmatrix}\lambda_{i,1} & \lambda_{i,2} & \dots & \lambda_{i,m}\end{bmatrix}$ be the $m$ eigenvalues of $H_i$ $(i = 1, 2)$. We can diagonalize $H_i$ by Fourier transform matrix as $H_i = \mathcal{F}^\dagger \Lambda_i \mathcal{F}$. Thus

$$\hat{\mathcal{H}} = \mathcal{F}^\dagger(\Lambda_1^\dagger\Lambda_1 + \Lambda_2^\dagger\Lambda_2)\mathcal{F}. \quad (20)$$

Let $\Lambda_1^\dagger\Lambda_1 + \Lambda_2^\dagger\Lambda_2 = \Lambda$, then $\Lambda$ has non-negative entries in the main diagonal and

$$\hat{\mathcal{H}}^{1/2} = \mathcal{F}^\dagger\Lambda^{1/2}\mathcal{F}, \quad (21a)$$

$$\hat{\mathcal{H}}^{-1/2} = \mathcal{F}^\dagger\Lambda^{-1/2}\mathcal{F}. \quad (21b)$$

We assume that $\boldsymbol{s}_i$ is pre-multiplied (or rotated) by a matrix $\mathcal{F}^\dagger$. Substituting $\boldsymbol{s}_i$ by $\mathcal{F}^\dagger\boldsymbol{s}_i$ and multiplying both sides of (19) with $\mathcal{F}$, one obtains

$$\begin{aligned}\Lambda^{-1/2}\mathcal{F}\hat{\boldsymbol{y}}_i &= \sqrt{\frac{\rho}{M}}\mathcal{F}\hat{\mathcal{H}}^{1/2}\mathcal{F}^\dagger\boldsymbol{s}_i + \Lambda^{-1/2}\mathcal{F}\hat{\boldsymbol{z}}_i\\ &= \sqrt{\frac{\rho}{M}}\Lambda^{1/2}\boldsymbol{s}_i + \underbrace{\Lambda^{-1/2}\mathcal{F}\hat{\boldsymbol{z}}_i}_{\check{\boldsymbol{z}}_i}. \end{aligned} \quad (22)$$

Since we can choose $\Lambda^{1/2}$ such that it has non-negative elements (in the main diagonal), the real and imaginary parts of $\boldsymbol{s}_i$ now can be separated for detection.

$$\Lambda^{-1/2}\Re(\mathcal{F}\hat{\boldsymbol{y}}_i) = \sqrt{\frac{\rho}{M}}\Lambda^{1/2}\Re(\boldsymbol{s}_i) + \Re(\check{\boldsymbol{z}}_i), \quad (23a)$$

$$\Lambda^{-1/2}\Im(\mathcal{F}\hat{\boldsymbol{y}}_i) = \sqrt{\frac{\rho}{M}}\Lambda^{1/2}\Im(\boldsymbol{s}_i) + \Im(\check{\boldsymbol{z}}_i). \quad (23b)$$

We finish deriving the general decoder for 4Gp-SAST codes. Using (23), one can use a sphere decoder to detect the transmitted symbols. The *equivalent channel* of 4Gp-SAST codes is $\Lambda^{1/2}$.

### C. Performance Analysis

Note that the eigenvalues of the $m \times m$ matrices $H_1$ and $H_2$ can be found easily using unnormalized Fourier transformation of the channel vectors $\boldsymbol{h}_1$ and $\boldsymbol{h}_2$ [19]. Therefore, the eigenvalues of $H_1$ and $H_2$ have distribution $\sim \mathcal{CN}(0, m)$.

We can introduce a real orthogonal transformation $R$ to the data vectors $\Re(\boldsymbol{s}_i)$ and $\Im(\boldsymbol{s}_i)$ $(i = 1, 2)$ to improve the performance of 4Gp-SAST codes. Thus the actual signal rotation of 4Gp-SAST codes is $\mathcal{F}^\dagger R$. Remember that the Fourier transform matrix $\mathcal{F}$ is used to make the equivalent channel of 4Gp-SAST codes real.

Since the PEP of vectors $\Re(\boldsymbol{s}_i)$ and $\Im(\boldsymbol{s}_i)$ $(i = 1, 2)$ are the same, we just calculate the PEP of the vector $\Re(\boldsymbol{s}_1)$. Let $\boldsymbol{d} = \Re(\boldsymbol{s}_1)\begin{bmatrix}a_1 & a_2 & \dots & a_m\end{bmatrix}^\mathsf{T}$.

The PEP of the pair $\boldsymbol{d}$ and $\bar{\boldsymbol{d}}$ can be expressed by the Gaussian tail function as [21]

$$P(\boldsymbol{d} \to \bar{\boldsymbol{d}}|\hat{\mathcal{H}}) = Q\left(\sqrt{\frac{\rho}{8}\frac{|\Lambda^{1/2}R\boldsymbol{\delta}|^2}{4N_0}}\right) \quad (24)$$

where $N_0 = 1/2$ is the variance of the elements of the white noise vector $\Re(\check{\boldsymbol{z}}_1)$ in (23a), $\boldsymbol{\delta} = \boldsymbol{d} - \bar{\boldsymbol{d}}$. Substituting $\Lambda = \Lambda_1^\dagger\Lambda_1 + \Lambda_2^\dagger\Lambda_2$, one has

$$\begin{aligned}P(\boldsymbol{d} \to \bar{\boldsymbol{d}}|\hat{\mathcal{H}}) &= Q\left(\sqrt{\frac{\rho\left[\boldsymbol{\delta}^\mathsf{T}R^\mathsf{T}(\Lambda_1^\dagger\Lambda_1 + \Lambda_2^\dagger\Lambda_2)R\boldsymbol{\delta}\right]}{16}}\right)\\ &= Q\left(\sqrt{\frac{\rho(\sum_{i=1}^{2}\sum_{j=1}^{m}\beta_j^2|\lambda_{i,j}|^2)}{16}}\right) \end{aligned} \quad (25)$$

where $\boldsymbol{\beta} = R\boldsymbol{\delta}$.

We now use the Craig's formula [22] to derive the conditional PEP in (24).

$$\begin{aligned}P(\boldsymbol{d} \to \bar{\boldsymbol{d}}|\hat{\mathcal{H}}) &= Q\left(\sqrt{\frac{\rho(\sum_{i=1}^{2}\sum_{j=1}^{m}\beta_j^2|\lambda_{i,j}|^2)}{16}}\right)\\ &= \frac{1}{\pi}\int_0^{\pi/2}\exp\left(\frac{-\rho(\sum_{i=1}^{2}\sum_{j=1}^{m}\beta_j^2|\lambda_{i,j}|^2)}{32\sin^2\alpha}\right)d\alpha. \end{aligned} \quad (26)$$

We can apply a method based on the moment generating function (MGF) [23], [24] to obtain the unconditional PEP in the following:

$$P(\boldsymbol{d} \to \bar{\boldsymbol{d}}) = \frac{1}{\pi} \int_0^{\pi/2} \left[ \prod_{i=1}^{m} \left( 1 + \frac{\rho \beta_i^2}{8 \sin^2 \alpha} \right) \right]^{-2} d\alpha. \quad (27)$$

Since there are four vectors to be decoded in each code matrix, the codeword PEP is therefore equal to 4 times the PEP given in (27).

Assume that $\beta_i \neq 0 \ \forall i = 1, 2, \ldots, m$. One can find the asymptotic PEP of 4Gp-SAST codes at high SNR as follows.

$$P(\boldsymbol{d} \to \bar{\boldsymbol{d}}) \approx \left( \frac{2^{6m} \rho^{-2m}}{\pi} \int_0^{\pi/2} (\sin \alpha)^{16} d\alpha \right) \prod_{i=1}^{m} \beta_i^{-4}$$
$$= \frac{2^{3M} \rho^{-M}}{2^{17}} \frac{16!}{8!8!} \prod_{i=1}^{M/2} \beta_i^{-4}. \quad (28)$$

The asymptotic bound in (28) shows an important property of the 4Gp-SAST codes at high SNR: The PEP is heavily dependent on the product distance $\prod_{i=1}^{4} \beta_i$ (see, e.g. [25]). The exponent of SNR in (28) is $-M$. This indicates that the maximum diversity order of 4Gp-QSTBC is 8 and it is achievable if the product distance is non-zero for all possible data vectors. Furthermore, at high SNR, the asymptotic bound becomes very tight to the exact PEP. Therefore, the larger the product distance, the lower FER can be obtained. Thus, we can optimize the rotation by $R$ so that the minimum product distance

$$d_{p,\min} = \min_{\forall \boldsymbol{d}^i, \boldsymbol{d}^j} \prod_{k=1}^{4} |\beta_k| \quad (29)$$

is non-zero and maximized.

For QAM signals, the symbols $a_i$ and $b_i$ are in the set $\{\pm 1, \pm 3, \pm 5, \ldots\}$, The best known rotations for QAM in terms of maximizing the minimum product distance are provided in [26], [27]; they are denoted by $R_{BOV}$.

In [26], [27], the rotated lattice points are generated by $\boldsymbol{x} = \boldsymbol{d} R_{BOV}$, where $\boldsymbol{d} \in \mathbb{Z}^n$ and $R_{BOV}$ is of size $m \times m$. In this representation, $\boldsymbol{x}$ and $\boldsymbol{d}$ are row vectors, while we use column vector notation in our paper. Thus the rotation matrices $R_{BOV}$ given in [26], [27] will be transposed. For the 3-dimensional lattices, the rotation matrix is given below.

$$R_{BOV,3} = \begin{bmatrix} -0.32798528 & -0.73697623 & -0.59100905 \\ -0.59100905 & -0.32798528 & 0.73697623 \\ -0.73697623 & 0.59100905 & -0.32798528 \end{bmatrix}. \quad (30)$$

Note that in the construction of 4Gp-SAST codes, the data vectors $\boldsymbol{s}_i$ $(i = 1, 2)$ with proper size are rotated to generate the vectors $\boldsymbol{u}_i$ as $\boldsymbol{u}_i = \mathcal{F}^\dagger R \boldsymbol{s}_i$.

## IV. Simulation Results

The performance of 4Gp-QSTBC and 4Gp-SAST codes will be compared with OSTBC [5], MDC-QSTBC [14], QSTBC [6], [28], 4Gp-QSTBC [16], DAST [11], and SAST codes [10].

### A. Performance of 4Gp-SAST codes for 6 antennas

Performance of 4Gp-SAST code for 6 antennas is compared with rate-2/3 OSTBC [5], and rate-one 4Gp-QSTBC and SAST codes in Fig. 1. In this simulation, the best 8QAM in terms of Euclidean distance [28] is selected for OSTBC, while 4QAM is for the other codes. Thus the bit rate of all the codes is 2 bits pcu. From Fig. 1, the 4Gp-SAST code perform significantly better than OSTBC (0.8 dB gain) and slightly worst than 4Gp-QSTBC and SAST codes. These results reflect the complexity-performance tradeoff (see also Table I).

### B. Performance of 4Gp-SAST codes for 8 antennas

We compare the performance of 4Gp-SAST codes with ABBA-QSTBC [6], [28] and MDC-QSTBC [14] for 8 antennas and spectral efficiency of 3 bits pcu in Fig. 2. To obtain 3 bits pcu, 16QAM is used with ABBA-QSTBC and MDC-QSTBC, while 8QAM is combined with 4Gp-SAST codes. For 8 antennas, the decoding of 4Gp-SAST codes require join detection of 4 real symbols, the same complexity of ABBA-QSTBC and higher than that of MDC-QSTBC. 4Gp-SAST codes perform much better than the two codes, due to higher code rate.

The performance of 4Gp-SAST codes is also compared with DAST codes [11] and 4Gp-QSTBC for the data rate of 4 bits pcu in Fig. 2. The decoding complexity of 4Gp-SAST codes for 8 antennas is the same as that of 4Gp-QSTBC (joint detection of 4 real symbols) and the two codes perform similarly. However, the decoding complexity of 4Gp-SAST is much lower than that of DAST (joint detection of 16 real symbols), but the former is superior to the latter. Nevertheless, SAST codes still perform better than 4Gp-SAST codes at the cost of higher complexity.

## V. Conclusions

We have presented 4Gp-SAST codes, a new class of four-group decodable STBC derived from SAST codes. The decoder of 4Gp-SAST codes is derived, enabling the derivation of the exact codeword pair-wise error probability. Therefore, the performance of 4Gp-SAST is optimized based on the exact PEP. The new codes are delay optimal for an even number of transmit antennas. This feature distinguishes the 4Gp-SAST codes from the previously known 4Gp-QSTBC, where the code length is a power of 2. Our 4Gp-SAST codes also perform better than several low complexity codes such as OSTBC, ABBA-QSTBC, MDC-QSTBC. The equivalent channel of 4Gp-SAST codes is provided in a simple diagonal form. Therefore, when certain kinds of channel state information are available at the transmitter, space-time precoder can be derived to further improve the performance of 4Gp-SAST codes. This problem can be a topic for future research.

## References

[1] A. Hottinen, O. Tirkkonen, and R. Wichman, *Multi-Antenna Transceiver Techniques for 3G and Beyond*. John Wiley & Sons, 2003.

[2] S. M. Alamouti, "A simple transmitter diversity scheme for wireless communication," *IEEE J. Select. Areas. Commun.*, vol. 16, pp. 1451–1458, Oct. 1998.

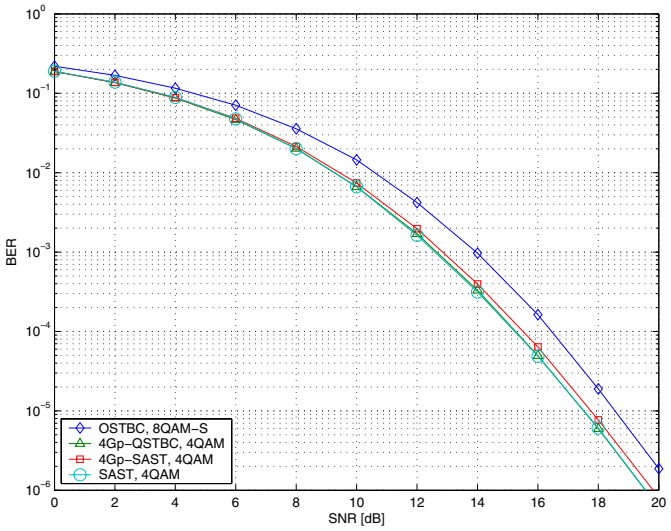


Fig. 1. Comparing performances of 4Gp-SAST codes with OSTBC and SAST codes, 6 transmit and 1 receive antennas, 2 bits pcu.

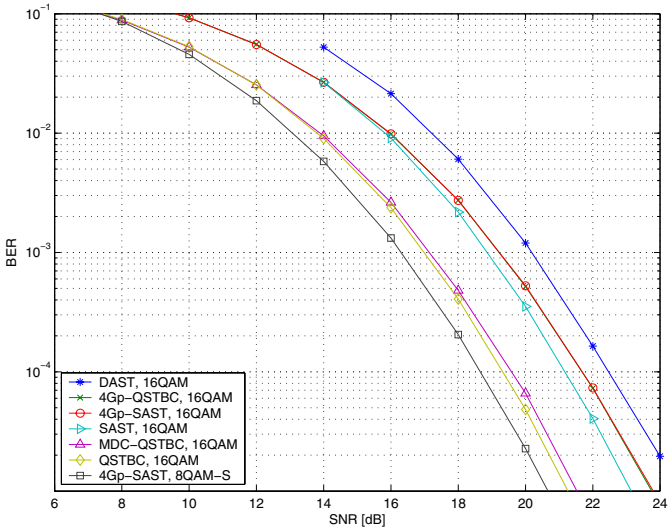


Fig. 2. Comparing performances of 4Gp-SAST codes with ABBA QSTBC, MDC-QSTBC, 4Gp-QSTBC, DAST and SAST codes, 8 transmit and 1 receive antennas, 3 and 4 bits pcu.

[3] V. Tarokh, H. Jafarkhani, and A. R.Calderbank, "Space-time block codes from orthogonal designs," *IEEE Trans. Inform. Theory*, vol. 45, pp. 1456–1466, July 1999.

[4] R. T. Derryberry, S. D. Gray, D. M. Ionescu, G. Mandyam, and B. Raghothaman, "Transmit diversity in 3G CDMA systems," *IEEE Commun. Mag.*, vol. 40, pp. 68–75, Apr. 2002.

[5] X.-B. Liang, "Orthogonal designs with maximal rates," *IEEE Trans. Inform. Theory*, vol. 49, pp. 2468 – 2503, Oct. 2003.

[6] O. Tirkkonen, A. Boariu, and A. Hottinen, "Minimal nonorthogonality rate 1 space-time block code for 3+ Tx antennas," in *Proc. IEEE 6th Int. Symp. Spread-Spectrum Techniques and Applications (ISSSTA 2000)*, Parsippany, NJ, USA, Sept. 2000, pp. 429–432.

[7] N. Sharma and C. B. Papadias, "Full-rate full-diversity linear quasi-orthogonal space-time codes for any number of transmit antennas," *EURASIP Journal on Applied Sign. Processing*, vol. 9, pp. 1246–1256, Aug. 2004.

[8] C. Yuen, Y. L. Guan and T. T. Tjhung, "Full-rate full-diversity STBC with constellation rotation," in *Proc. IEEE Vehicular Technology Conf. (VTC)*, April 22-25 2003, pp. 296 – 300.

[9] L. Xian and H. Liu, "Rate-one space-time block codes with full diversity," *IEEE Trans. Commun.*, vol. 53, pp. 1986 – 1990, Dec. 2005.

[10] D. N. Đào and C. Tellambura, "Capacity-approaching semi-orthogonal space-time block codes," in *Proc. IEEE GLOBECOM*, St. Louis, MO, USA, Nov./Dec. 2005.

[11] M. O. Damen, K. Abed-Meraim and J. -C. Belfiore, "Diagonal algebraic space-time block codes," *IEEE Trans. Inform. Theory*, vol. 48, pp. 628 – 636, March 2002.

[12] Y. Xin, Z. Wang, and G. B. Giannakis, "Space-time diversity systems based on linear constellation precoding," *IEEE Trans. Wirel. Commun.*, vol. 2, pp. 294 – 309, March 2003.

[13] M. Z. A. Khan and B. S. Rajan, "Single-symbol maximum likelihood decodable linear STBCs," *IEEE Trans. Inform. Theory*, vol. 52, pp. 2062 – 2091, May 2006.

[14] C. Yuen, Y. L. Guan, and T. T. Tjhung, "Quasi-orthogonal STBC with minimum decoding complexity," *IEEE Trans. Wirel. Commun.*, vol. 4, pp. 2089 – 2094, Sep. 2005.

[15] ——, "On the search for high-rate quasi-orthogonal space-time block code," *International Journal of Wireless Information Network (IJWIN)*, to appear. [Online] Available: dx.doi.org/10.1007/s10776-006-0033-2.

[16] ——, "A class of four-group quasi-orthogonal space-time block code achieving full rate and full diversity for any number of antennas," in *Proc. IEEE Personal, Indoor and Mobile Radio Communications Symp. (PIMRC)*, Berlin, Germany, Sep. 2005.

[17] R. A. Horn and C. R. Johnson, *Matrix Analysis*. Cambridge, U.K.: Cambridge Univ. Press, 1985.

[18] B. Hassibi and B. M. Hochwald, "High-rate codes that are linear in space and time," *IEEE Trans. Inform. Theory*, vol. 48, pp. 1804–1824, July 2002.

[19] P. J. Davis, *Circulant Matrices*, 1st ed. Newyork: Wiley, 1979.

[20] M. O. Damen, H. El Gamal and G. Caire, "On maximum-likelihood detection and the search for the closest lattice point," *IEEE Trans. Inform. Theory*, vol. 49, pp. 2389 – 2402, Oct. 2003.

[21] J. G. Proakis, *Digital Communications*, 4th ed. New York: McGraw-Hill, 2001.

[22] J. W. Craig, "A new, simple and exact result for calculating the probability of error for two-dimensional signal constellations," in *Proc. IEEE Military Communications Conf. (MILCOM)*, Boston, MA, USA, Nov. 1991, pp. 25.5.1 – 25.5.5.

[23] C. Tellambura, A. J. Mueller and V. K. Bhargava, "Analysis of M-ary phase-shift keying with diversity reception for land-mobile satellite channels," *IEEE Trans. Veh. Technol.*, vol. 46, pp. 910–922, Nov. 1997.

[24] M. K. Simon and M.-S. Alouini, *Digital Communication over Fading Channels*, 1st ed. New York: Wiley, 2000.

[25] J. Boutros and E. Viterbo, "Signal space diversity: A power and bandwidth efficient diversity technique for the Rayleigh fading channel," *IEEE Trans. Inform. Theory*, vol. 44, pp. 1453 – 1467, July 1998.

[26] E. Bayer-Fluckiger, F. Oggier, and E. Viterbo, "New algebraic constructions of rotated $Z^n$-lattice constellations for the Rayleigh fading channel," *IEEE Trans. Inform. Theory*, vol. 50, pp. 702 – 714, April 2004.

[27] F. Oggier and E. Viterbo, Full Diversity Rotations. [Online]. Available: www1.tlc.polito.it/∼viterbo/rotations/rotations.html.

[28] W. Su and X.-G. Xia, "Signal constellations for quasi-orthogonal space-time block codes with full diversity," *IEEE Trans. Inform. Theory*, vol. 50, pp. 2331 – 2347, Oct. 2004.